NASA Technical Memorandum 107151

Application of the Self Calibrating Emissivity and/or Transmissivity Independent Multiwavelength Pyrometer in an Intense Ambient Radiation Environment

Daniel Ng
Lewis Research Center
Cleveland, Ohio

January 1996

National Aeronautics and
Space Administration

APPLICATION OF THE SELF CALIBRATING EMISSIVITY AND/OR TRANSMISSIVITY INDEPENDENT MULTIWAVELENGTH PYROMETER IN AN INTENSE AMBIENT RADIATION ENVIRONMENT

DANIEL NG
NASA Lewis Research Center
Cleveland, OH 44135

Introduction

The NASA self calibrating multiwavelength pyrometer[1] is a recent addition to the list of pyrometers used in remote temperature measurement in research and development. The older one-color, two-color and the disappearing filament pyrometers[2] as well as the multicolor and early multiwavelength pyrometers[3-5] all do not operate successfully in situations in which strong ambient radiation coexist with radiation originating from the measured surface. Figure 1 depicts the situation in question. Radiation departing from the target surface arrives at the pyrometer together with radiation coming from another source either directly or through reflection. Unlike the other pyrometers, the self calibrating multiwavelength pyrometer can still calibrate itself and measure the temperatures in this adverse environment.

Theory

In reference 1, it was shown that voltage spectra measured by a pyrometer contain enough information to determine all the quantities necessary for pyrometry. The voltage spectra $V(\lambda,T(t))$ are of wavelengths $\lambda_1, \lambda_2, ..\lambda_s.. \lambda_N$, N>2, at times $t_1, t_2, .. t_i, .. t_n$, though measured at unknown temperatures $T(t_1)\neq T(t_2)\neq .. \neq T(t_i)\neq ..\neq T(t_n)$, with unknown target surface spectral emissivity ε_λ, unknown optical medium transmissivity τ_λ between the measured surface and the pyrometer, and unknown instrument calibration constant g_λ, all these unknowns as well as the unknown temperatures can be determined. The bases of the self calibrating pyrometer is contained in three equations[1] (Eqns. 1-3) connecting two 2 wavelengths, labeled λ_R and λ_I.

$$\frac{c_1}{\lambda_i^5}\frac{1}{V(\lambda_I,t)}=\frac{1}{g_I\varepsilon_I\tau_I}\left\{\left(g_R\varepsilon_R\tau_R\frac{c_1}{\lambda_R^5}\frac{1}{V(\lambda_R,t)}+1\right)^{\frac{\lambda_R}{\lambda_I}}\right\}-\frac{1}{g_I\varepsilon_I\tau_I} \tag{1}$$

$$T(\lambda,t)=\frac{c_2/\lambda_I}{Log_e\left(g_I\varepsilon_I\tau_I\frac{c_1}{\lambda_I^5}\frac{1}{V(\lambda_I,t)}+1\right)} \tag{2}$$

$$T(t)=\frac{\sum_{I=1}^{I=N}T(\lambda_I,t)}{N} \tag{3}$$

With the determination of a single number, $g_R\varepsilon_R\tau_R$, all the other $g_I\varepsilon_I\tau_I$ and temperatures T(t) are automatically determined. $g_R\varepsilon_R\tau_R$ is determined using a least squares variational method, beginning by assuming a value for $g_R\varepsilon_R\tau_R$, plotting the quantity on the left hand side of Eqn. 1 vs the quantity inside the curly bracket on the right hand side to obtain a straight line, the slope gives $g_I\varepsilon_I\tau_I$. Do this for all I≠R to determine $g_I\varepsilon_I\tau_I$ and use them to calculate the average temperatures T(t).

In the application of this multiwavelength pyrometer to the geometry of figure 1, because of the presence of the ambient radiation, the voltage spectrum, now denoted by $S(\lambda,t)$ is given in Eqn. 4.

$$S(\lambda,t) = g_\lambda \left(\varepsilon_\lambda \tau_\lambda \frac{C_1}{\lambda^5} \frac{1}{\exp(c_2/\lambda T(t)) - 1} + I(\lambda,t) \right)$$
$$= g_\lambda \varepsilon_\lambda \tau_\lambda \left(\frac{C_1}{\lambda^5} \frac{1}{\exp(c_2/\lambda T(t)) - 1} + \frac{1}{\varepsilon_\lambda \tau_\lambda} I(\lambda,t) \right) \quad (4)$$
$$= g_\lambda \varepsilon_\lambda \tau_\lambda \left(\frac{C_1}{\lambda^5} \frac{1}{\exp(c_2/\lambda T(t) - 1} + I'(\lambda,t) \right)$$

$I(\lambda,t)$ is the spectral intensity of the ambient radiation and $I'(\lambda,t)$ is a transformation obtained from it. If $I(\lambda,t)$ and hence $I'(\lambda,t)$ is slowly and randomly varying with time, then the quantity $V(\lambda,t)$, in Eqns. 1 to 3, intrinsically related to the temperature of the measured surface can be recovered and used to determine the relevant g, ε, τ and hence the temperatures T(t) by the following steps:

S1: Beginning with t=0, a difference spectrum $D(\lambda,t_1,0)$ is formed according to Eqn. 5, between the first and second measurement.

$$D(\lambda, t_1, t_0=0) = (S(\lambda, t_1) - S(\lambda, t_0=0))$$
$$= g_\lambda \varepsilon_\lambda \tau_\lambda \left[\frac{C_1}{\lambda^5} \frac{1}{\exp(c_2/\lambda T(t_1)) - 1} - \frac{C_1}{\lambda^5} \frac{1}{\exp(c_2/\lambda T(t_0=0)) - 1} + I'(\lambda, t_1) - I'(\lambda, t_0=0) \right] \quad (5)$$

More generally the difference spectrum $D(\lambda,t_i,t_{i-1})$ is defined iteratively in Eqn. 6.

$$D(\lambda, t_i, t_{i-1}) = (S(\lambda, t_i) - S(\lambda, t_{i-1}))$$
$$= g_\lambda \varepsilon_\lambda \tau_\lambda \left[\frac{C_1}{\lambda^5} \frac{1}{\exp(c_2/\lambda T(t_i)) - 1} - \frac{C_1}{\lambda^5} \frac{1}{\exp(c_2/\lambda T(t_{i-1})) - 1} + I'(\lambda, t_i) - I'(\lambda, t_{i-1}) \right] \quad (6)$$

S2: Form the sum of the difference spectra from t=0 to $t=t_i$ according to Eqn. 7.

$$\sum_{i=1}^{i} D(\lambda, t_i, t_{i-1}) = (S(\lambda, t_i) - S(\lambda, t=0))$$
$$= g_\lambda \varepsilon_\lambda \tau_\lambda \left[\frac{C_1}{\lambda^5} \frac{1}{\exp(c_2/\lambda T(t_i)) - 1} - \frac{C_1}{\lambda^5} \frac{1}{\exp(c_2/\lambda T(t=0)) - 1} + I'(\lambda, t_i) - I'(\lambda, t=0) \right] \quad (7)$$

S3: Choose a reference time t_r. At this time the temperature is T_r. Analogous to Eqn. 7, define the sum of the difference spectra from t=0 to $t=t_r$ in Eqn. 8.

$$\sum_{i=1}^{i=r} D(\lambda, t_i, t_{i-1}) = (S(\lambda, t_r) - S(\lambda, t=0))$$
$$= g_\lambda \varepsilon_\lambda \tau_\lambda \left[\frac{C_1}{\lambda^5} \frac{1}{\exp(c_2/\lambda T(t_r)) - 1} - \frac{C_1}{\lambda^5} \frac{1}{\exp(c_2/\lambda T(t=0)) - 1} + I'(\lambda, t_r) - I'(\lambda, t=0) \right] \quad (8)$$

S4: The difference between Eqn. 7 and Eqn. 8 (Eqn. 9) is the sum of all the difference spectra between $t=t_r$ and $t=t_i$

$$\Delta V(\lambda, t_i) = \sum_{i=1}^{i} D(\lambda, t_i, t_{i-1}) - \sum_{i=1}^{r} D(\lambda, t_i, t_{i-1}) = (S(\lambda, t_i) - S(\lambda, t_r))$$
$$= g_\lambda \varepsilon_\lambda \tau_\lambda \left[\frac{C_1}{\lambda^5} \frac{1}{\exp(c_2/\lambda T(t_i)) - 1} - \frac{C_1}{\lambda^5} \frac{1}{\exp(c_2/\lambda T(t_r)) - 1} + I'(\lambda, t_i) - I'(\lambda, t_r) \right] \quad (9)$$

S5: This is rearranged in Eqn. 10.

$$g_\lambda \varepsilon_\lambda \tau_\lambda L(\lambda, t_i) = g_\lambda \varepsilon_\lambda \tau_\lambda L(\lambda, t_r) + \Delta S(\lambda, t_i) + \Delta I'(\lambda, t_i) \qquad (10)$$

where $L(\lambda,t)$ is the Planck formula, and $\Delta S(\lambda,t_i)$, $\Delta I'(\lambda,t_i)$ are defined as

$$\begin{aligned} \Delta S(\lambda, t_i) &= S(\lambda, t_i) - S(\lambda, t_r) \\ \Delta I'(\lambda, t_i) &= I'(\lambda, t_i) - I'(\lambda, t_r) \end{aligned} \qquad (11)$$

S6: For constant or slowly and randomly varying $I(\lambda,t)$, $\Delta I'(\lambda,t)=0$, Eqn. 10 becomes

$$g_\lambda \varepsilon_\lambda \tau_\lambda L(\lambda, t_i) = g_\lambda \varepsilon_\lambda \tau_\lambda L(\lambda, t_r) + \Delta S(\lambda, t_i) \qquad (12)$$

$g_\lambda \varepsilon_\lambda \tau_\lambda L(\lambda,t_i)$ is the voltage spectrum that the pyrometer would have detected at t_i in the absence of the ambient radiation $I(\lambda,t_i)$, and it equals $g_\lambda \varepsilon_\lambda \tau_\lambda L(\lambda,t_r)$, the voltage spectrum that the pyrometer would have detected at time t_r in the absence of the ambient radiation plus $\Delta S(\lambda,t_i)$, the increase in the sum of difference spectra when the target temperature has changed from $T(t_r)$ to $T(t_i)$ between time t_r and time t_i. The expression for $V(\lambda,t)$ is now given by Eqn. 13.

$$V(\lambda, t_i) = g_\lambda \varepsilon_\lambda \tau_\lambda L(\lambda, t_r) + \Delta S(\lambda, t_i) \qquad (13)$$

Experiment and Results

The voltages $V(\lambda,t)$ in Eqns. 1 to 3 in the derivation of the self-calibrating multiwavelength pyrometer in reference 1 are now given by Eqn. 13. By direct substitution and minor modification, using difference spectra obtained in steps (S1 to S6) are processed to determine the unknown temperatures and all the necessary calibration constants. Substituting Eqn. 13 in Eqn. 1 and rearranging gives Eqn. 14.

$$\Delta S(\lambda_I, t) = g_I \varepsilon_I \tau_I \left\{ \frac{\frac{C_1}{\lambda_I^5}}{\left(\frac{C_1/\lambda_R^5}{L(\lambda_R, T_r) + \Delta S(\lambda_R, t)/g_R \varepsilon_R \tau_R} + 1 \right)^{\frac{\lambda_R}{\lambda_I}} - 1} \right\} - g_I \varepsilon_I \tau_I L(\lambda_I, T_r) \qquad (14)$$

Referring to Eqn. 14, assign a value for $g_R \varepsilon_R \tau_R$ and a value for T_r, evaluate the quantity inside the curly bracket on the right hand side and use it to plot against the quantity on the left hand side of it. A straight line is obtained. Standard least squares method is used to determine its slope, which is $g_I \varepsilon_I \tau_I$. Another least squares procedure is used to determine $g_R \varepsilon_R \tau_R$ and T_r as follows:

1) Choose a value for T_r.
2) Choose a wavelength for λ_R and a wavelength for λ_I and a value for $g_R \varepsilon_R \tau_R$.
3) Plot the data according to Eqn 14 to determine the $g_I \varepsilon_I \tau_I$ from the slopes.
4) Do so for all $I \neq R$.
5) Use the so determined $g_I \varepsilon_I \tau_I$ to calculate the temperatures $T(t)$ according to Eqns. 2, 3 and 13.
6) Transform the spectra $V(\lambda_I,t)$ into a single large data set (x,y). The wavelength λ_I is transformed into $c_2/\lambda_I T(t)$, the transformed wavelength, the voltage $V(\lambda_I,t)$ is transformed by first dividing by $g_I \varepsilon_I \tau_I$ and then by $T(t)^5$, the 5th power of the spectrum temperature, according to the prescription

$$x = \frac{c_2}{\lambda T(t)} \quad , \quad y = \frac{V(\lambda, t)}{A} \frac{1}{T(t)^5} = \frac{c_1}{c_2^5} \frac{x^5}{e^x - 1} \qquad (15)$$

7) The transformed (x,y) data obey the generalized non-dimensional Planck function. The (x,y) data are fitted to the Planck function in Eqn. 15 by calculating the residual Σ, defined as the sum of the squares of the difference between the transformed y_I and the calculated y evaluated

by substituting the transformed x_I in the y equation in Eqn 15 for all the data.

8) A new value for $g_R\varepsilon_R\tau_R$ is selected, and steps (2 to 7) repeated.

9) The value of $g_R\varepsilon_R\tau_R$ that produced the least Σ is recorded.

10) Choose a new value for T_r, repeat steps (2 to 9).

11) The combination of $g_R\varepsilon_R\tau_R$ and T_r that produced the least over all Σ is the correct one we are after.

When $g_R\varepsilon_R\tau_R$, T_r are determined, the other T(t) are also determined. In one stroke, everything that is needed in pyrometry for temperature measurement is determined. Temperatures at any time in the past or in the future are determined from each λ according to Eqn 3 or by least squares curve fitting. As is evident, the pyrometer requires no prior calibration. The procedures (1 to 11) can be repeated as often as necessary during an experiment to update the self calibrating process.

A simulation experiment of the condition in figure 1 is shown in figure 2. It consisted of a black body furnace and the spectrometer of a multiwavelength pyrometer; between them were placed a quartz lamp and a slab of transmitting material (zinc selenide, ZnSe). This transmitting material was polished so that it possessed optical quality parallel surfaces. It was then positioned between the quartz lamp and the spectrometer so that the black body radiation transmitted through it, and the quartz lamp radiation, specularly reflected, would arrive and mix at the pyrometer detector. The ZnSe-transmitted black body radiation simulated the target surface radiation; the ZnSe transmissivity is unknown and simulated the target surface emissivity; the more intense, specularly reflected quartz lamp radiation in this simulation replaced the weaker, diffusely reflected ambient radiation normally would be encounter in an actual experiment. The quartz lamp emitted (1) short wavelength ($\lambda < 2.5$ μm) radiation transmitted from the filament through its envelope and (2) longer wavelength radiation emitted by the envelope after its temperature had increased.

In this experiment, the spectrometer of a multiwavelength pyrometer recorded a series of spectra. A stable power supply generated a constant current through the quartz lamp filament to produce a constant radiation flux. The temperature of the black body furnace was gradually increased. The black body furnace temperature was measured using a type G thermocouple. The TC measured black body furnace temperatures are 763, 871, 984, 1101, 1224 and 1351 K. Six of the changing spectra are shown in figure 3. These spectra spanned the spectral region from 1.3 to 14.5 μm. It recorded the direct voltage output of the indium antimonide and mercury cadmium telluride detectors.

Results The spectrum minima in figure 3 are due to atmospheric CO_2 and H_2O absorptions in the optical path between the detector and the black body source. One of the spectra in figure 3 is chosen as the reference, it is subtracted from the other spectra, including itself. The difference spectra so generated are shown in figure 4. Following the analysis above, λ_R is chosen to be 5 μm. An arbitrary initial value for $g_R\varepsilon_R\tau_R$ is used, plots according to Eqn. 14 are made. Figure 5 shows the case for λ_R=5 μm, and λ_I=2 μm, $g_R\varepsilon_R\tau_R$=1.6468, and T_r=1224 K. It is indeed a straight line. The slope (i.e. $g_I\varepsilon_I\tau_I$) of plots like this at other wavelengths are obtained using least squares method. They are plotted in fig. 6. These $g_I\varepsilon_I\tau_I$ are now used to calculate the temperature of each spectrum according to Eqn. 2. The intrinsic voltages are given by Eqn. 13, and the calculated temperatures are shown in fig. 7. They are almost independent of wavelength. The explosion at the shortest wavelength and low temperatures are due to poor signal to noise there. At some wavelengths, there is no solution to Eqn. 2 which involves the logarithm. When data at these wavelengths are excluded, averages are obtained according to Eqn. 3. These averages, and everything that depends on $g_R\varepsilon_R\tau_R$ change when $g_R\varepsilon_R\tau_R$ takes on different values. Of the many possible values that $g_R\varepsilon_R\tau_R$ can assume, we identify the correct one using the least squares curve fitting procedure described in steps 1 to 11. Least squares fitting of the transformed data to the non-dimensional Planck formula is shown in figure 8. The agreement is excellent.

Once the value of $g_R\varepsilon_R\tau_R$ and T_r are fixed, the values of all other $g_I\varepsilon_I\tau_I$ and the temperatures of the other spectra are fixed as a consequence. These temperatures are 750, 864, 981, 1101, 1224 and 1354 K. The pyrometry measured temperatures and the TC measured temperatures are compared in fig. 9. They differ by less then 2%. Obviously the pyrometer measured these temperatures without having

been previously calibrated.

Four of the 445 wavelengths were selected for a similar analysis, a smaller (x,y) data set is now generated. These wavelengths were 2.4, 3, 4 and 5 μm. The value of $g_R\varepsilon_R\tau_R$ that produced the least squares is 1.647, almost exactly the same as before. The resulting fit of the data to the generalized Planck function is performed and shown in figure 10. The temperatures determined were also almost exactly the same. The choice of these 4 wavelengths occur in the regions where the signal is strongest in the temperature range that measurements were made.

Conclusion

The multiwavelength pyrometer successfully measured the temperatures of a black body furnace viewed through a transparent window of unknown transmissivity, in the presence of constant or slowly and randomly varying strong ambient radiation. The measurement error is less than 2%. This is significant because the pyrometer is not previously calibrated with a standard such as a black body furnace. The use of only 4 wavelengths in the most optimal spectral regions produced almost identical results, reducing the amount of data and data acquisition time by a factor of over 100.

Reference

1 Ng, Daniel, Self Calibrating emissivity and/or transmissivity independent multiwavelength pyrometer, NASA TM107149 E-Number 10087, 1996.

2 DeWitt, D.P., Nutter, G.D., Theory and Practice of Radiation Thermometry, John Wiley & Sons, New York, 1988.

2. Hunter, G.B.; Allemand, C; and Eagar, T.W., Multiwavelength Pyrometer - An Improved Method., Opt. Eng., vol. 24, no. 6, Nov.-Dec. 1985, pp. 1081-1085.

3. Ng, Daniel, Williams, W.D., "Full spectrum pyrometry for nongray surface in the presence of interfering radiation", Temperature, Its Measurement and Control in Science and Industry, James F. Schooley Editor, Volume 6, American Institute of Physics, pp 889-894.

4. Ng, Daniel, "A Self-Calibrating, Emissivity Independent Multiwavelength Pyrometer", NASA Conference Publication 10146, 1994, page 28-1 to 28-10.

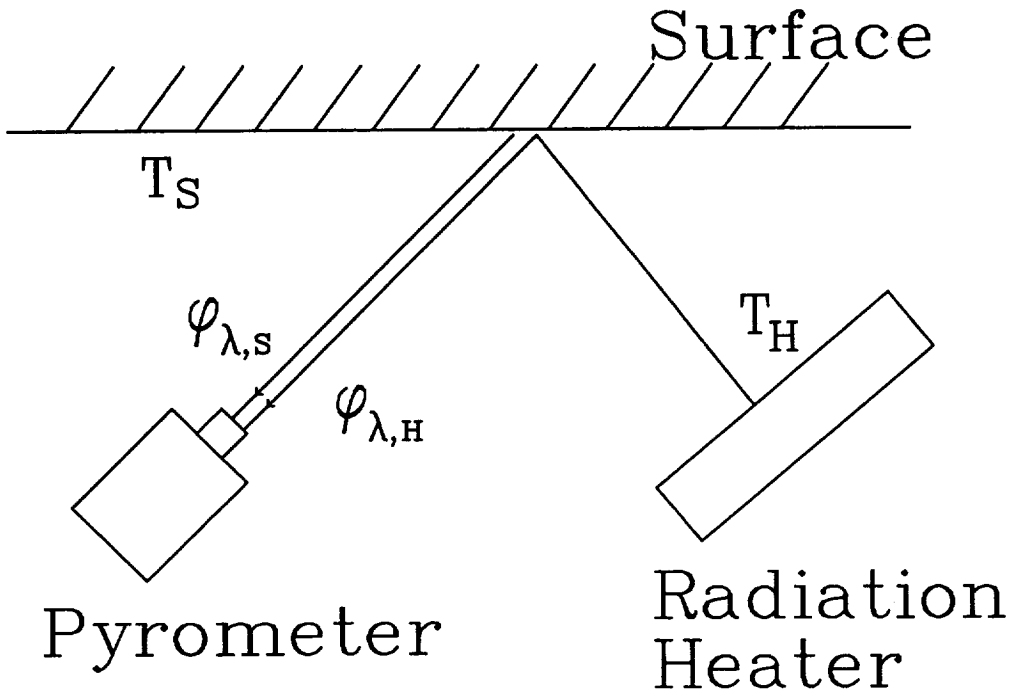

Figure 1

Pyrometer Arrangement in a Ceramics Application.

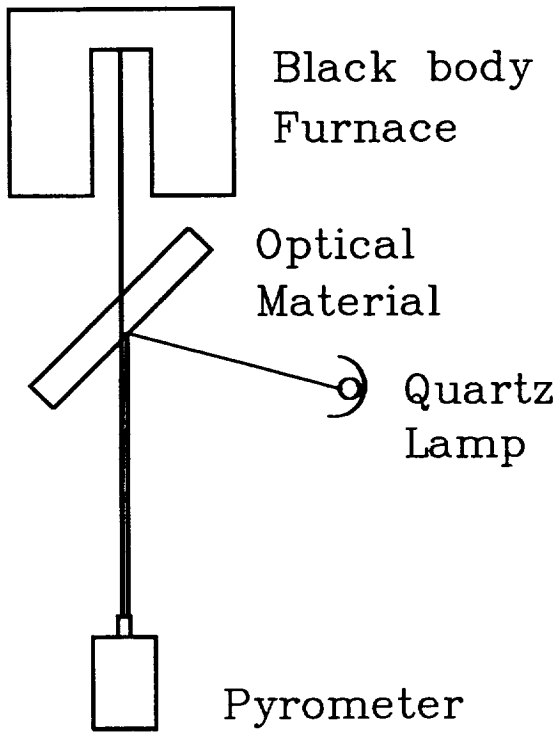

Figure 2

Arrangement for Simulation Experiment.

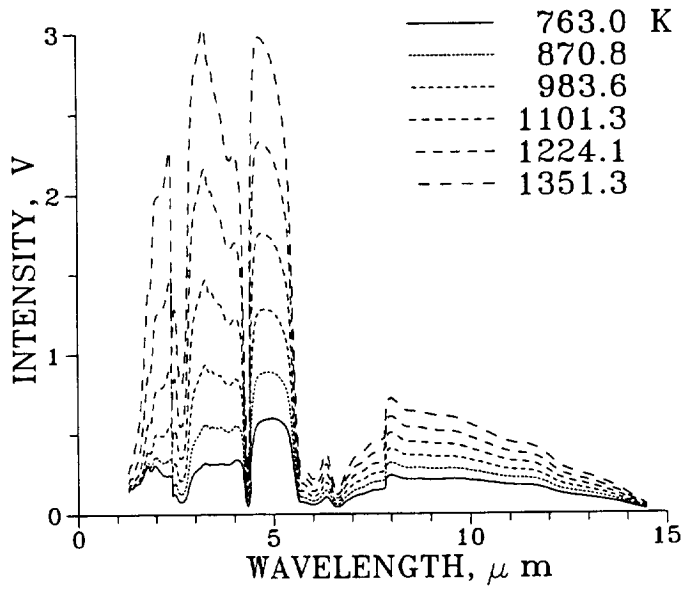

Figure 3

Spectra of Simulated Quartz-heated Surface.

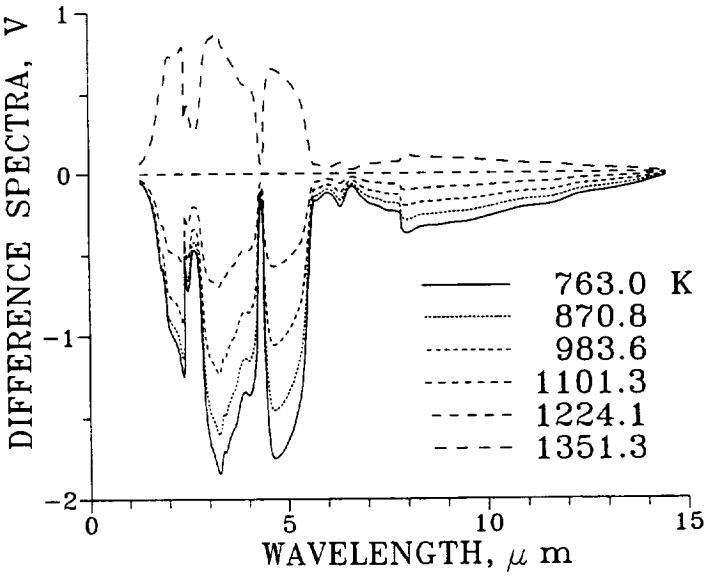

Figure 4

Difference spectra obtained by subtracting a chosen reference from the other spectra.

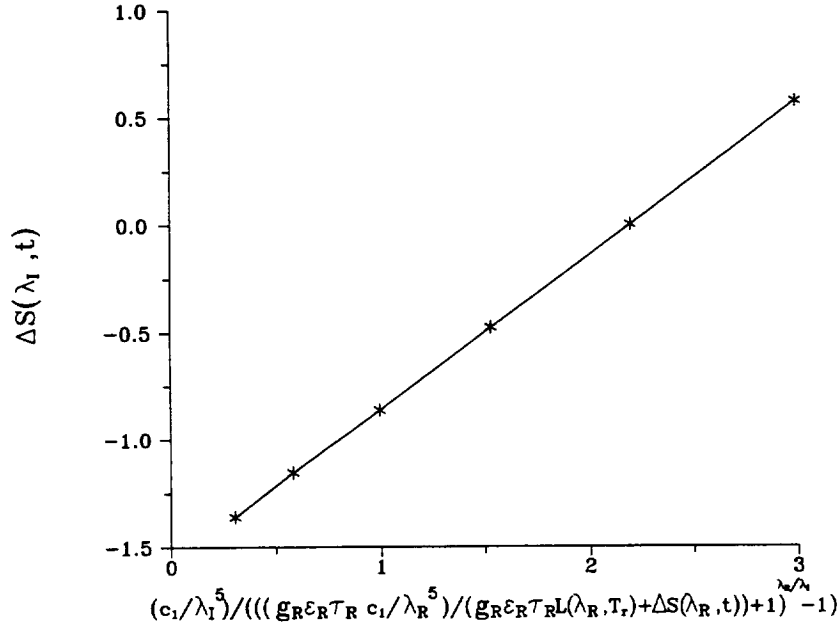

Figure 5
Plot of data to determine slope according to Eqn 14, λ_I=2 μm, λ_R=5 μm, T_r=1224 K.

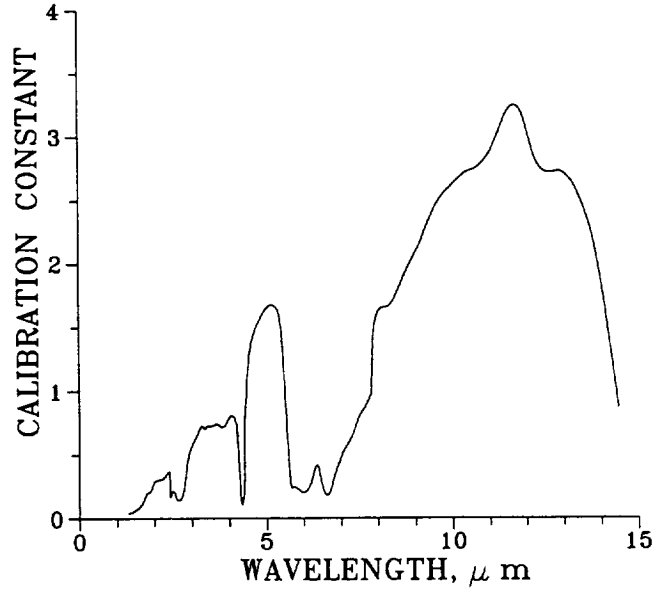

Figure 6
Calibration constants.

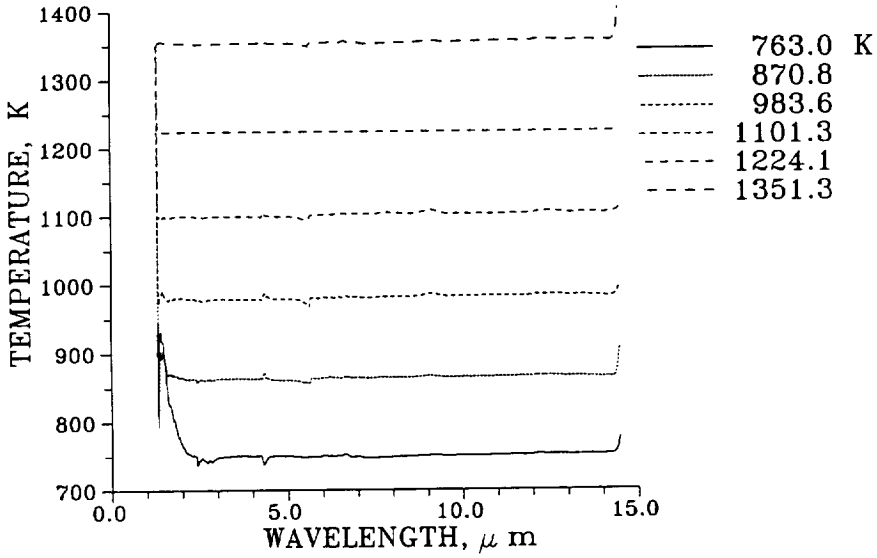

Figure 7
Calculated temperatures use the determined calibration constants.

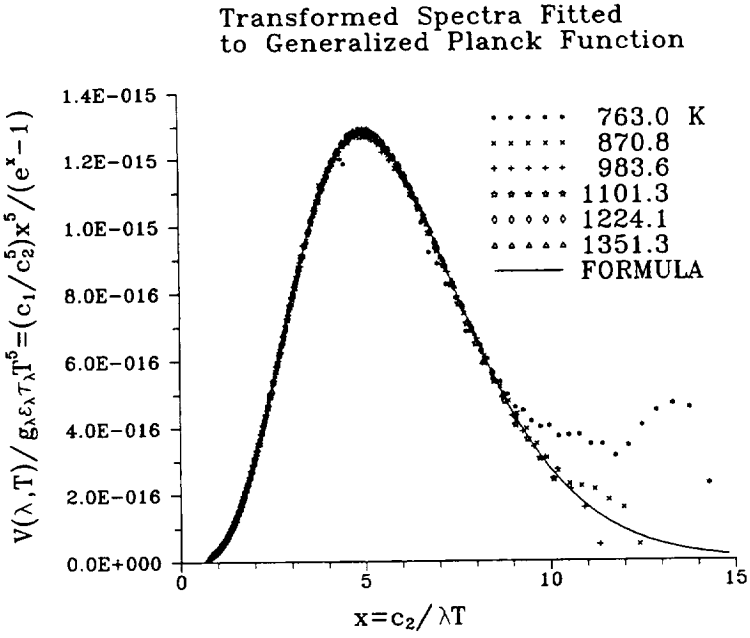

Figure 8
Least squares curve fitting of the transformed data to the non-dimensional Planck function.

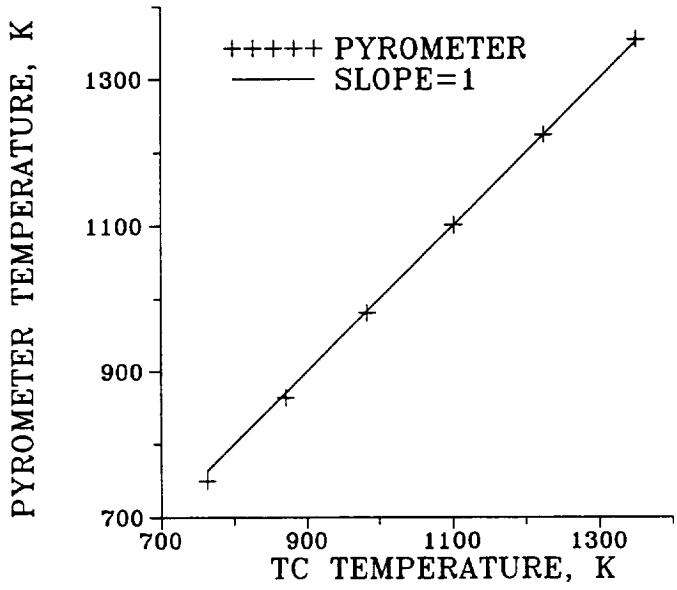

Figure 9
Plot of pyrometer measured temperature vs thermocouple measured temperature.

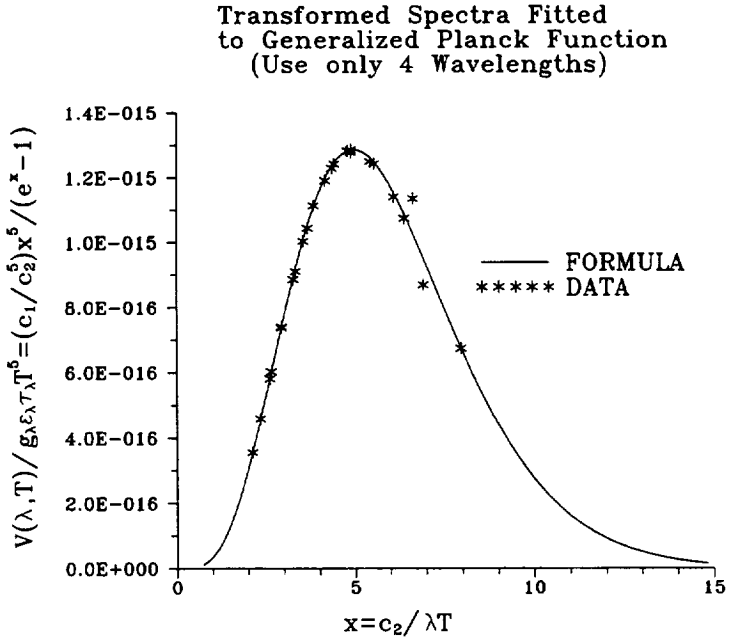

Figure 10
Fit of data from 4 wavelengths to the non-dimensional Planck Equation.

REPORT DOCUMENTATION PAGE

Form Approved
OMB No. 0704-0188

1. AGENCY USE ONLY (*Leave blank*)	2. REPORT DATE	3. REPORT TYPE AND DATES COVERED
	January 1996	Technical Memorandum

4. TITLE AND SUBTITLE

Application of the Self Calibrating Emissivity and/or Transmissivity Independent Multiwavelength Pyrometer in an Intense Ambient Radiation Environment

5. FUNDING NUMBERS

WU-505-62-50

6. AUTHOR(S)

Daniel Ng

7. PERFORMING ORGANIZATION NAME(S) AND ADDRESS(ES)

National Aeronautics and Space Administration
Lewis Research Center
Cleveland, Ohio 44135-3191

8. PERFORMING ORGANIZATION REPORT NUMBER

E-10089

9. SPONSORING/MONITORING AGENCY NAME(S) AND ADDRESS(ES)

National Aeronautics and Space Administration
Washington, D.C. 20546-0001

10. SPONSORING/MONITORING AGENCY REPORT NUMBER

NASA TM-107151

11. SUPPLEMENTARY NOTES

Responsible person, Daniel Ng, organization code 2510, (216) 433-3638.

12a. DISTRIBUTION/AVAILABILITY STATEMENT

Unclassified - Unlimited
Subject Category 35

This publication is available from the NASA Center for Aerospace Information, (301) 621-0390.

12b. DISTRIBUTION CODE

13. ABSTRACT (*Maximum 200 words*)

The NASA self calibrating multiwavelength pyrometer is a recent addition to the list of pyrometers used in remote temperature measurement in research and development. The older one-color, two-color, and the disappearing filament pyrometers as well as the multicolor and early multiwavelength pyrometers all do not operate successfully in situations in which strong ambient radiation coexist with radiation originating from the measured surface. Figure 1 depicts the situation in question. Radiation departing from the target surface arrives at the pyrometer together with radiation coming from another source either directly or through reflection. Unlike the other pyrometers, the self calibrating multiwavelength pyrometer can still calibrate itself and measure the temperatures in this adverse environment.

14. SUBJECT TERMS	15. NUMBER OF PAGES
Pyrometry; Emissivity; Interference; Radiation	12
	16. PRICE CODE: A03

17. SECURITY CLASSIFICATION OF REPORT	18. SECURITY CLASSIFICATION OF THIS PAGE	19. SECURITY CLASSIFICATION OF ABSTRACT	20. LIMITATION OF ABSTRACT
Unclassified	Unclassified	Unclassified	

National Aeronautics and
Space Administration

Lewis Research Center
21000 Brookpark Rd.
Cleveland, OH 44135-3191